ARMY RESEARCH LABORATORY

Validated Antenna Models for Standard Gain Horn Antennas

By Christos E. Maragoudakis and Edward Rede

ARL-TN-0371 September 2009

NOTICES

Disclaimers

Army Research Laboratory
White Sands Missile Range, NM 88002-5513

ARL-TN-0371 **September 2009**

Validated Antenna Models for Standard Gain Horn Antennas

Christos E. Maragoudakis and Edward Rede
Survivability/Lethality Analysis Directorate, ARL

REPORT DOCUMENTATION PAGE					*Form Approved OMB No. 0704-0188*

1. REPORT DATE *(DD-MM-YYYY)* September 2009	**2. REPORT TYPE** Final	**3. DATES COVERED (From - To)** February 1, 2009–March 31, 2009
4. TITLE AND SUBTITLE Validated Antenna Models for Standard Gain Horn Antennas		**5a. CONTRACT NUMBER**
		5b. GRANT NUMBER
		5c. PROGRAM ELEMENT NUMBER
6. AUTHOR(S) Christos E. Maragoudakis and Edward Rede		**5d. PROJECT NUMBER**
		5e. TASK NUMBER
		5f. WORK UNIT NUMBER
7. PERFORMING ORGANIZATION NAME(S) AND ADDRESS(ES) U.S. Army Research Laboratory Information and Electronic Protection Division Survivability/Lethality Analysis Directorate (ATTN: RDRL-SLE-S) White Sands Missile Range, NM 88002-5513		**8. PERFORMING ORGANIZATION REPORT NUMBER** ARL-TN-0371
9. SPONSORING/MONITORING AGENCY NAME(S) AND ADDRESS(ES)		**10. SPONSOR/MONITOR'S ACRONYM(S)**
		11. SPONSOR/MONITOR'S REPORT NUMBER(S)

12. DISTRIBUTION/AVAILABILITY STATEMENT

Approved for public release; distribution is unlimited.

13. SUPPLEMENTARY NOTES

14. ABSTRACT

Developed radiation pattern models of standard gain horn antennas using High Frequency Structure Simulator (HFSS) software are presented in this technical note. The models were validated using data measured in an anechoic chamber. Comparison tables of the beamwidth, sidelobe level and first null beamwidth of the measured and modeled radiation patterns for E-plane and H-plane patterns are also presented. Finally, figures depicting the measured and modeled antenna patterns are shown in the appendix.

15. SUBJECT TERMS

Radiation patterns, horn antennas, Model, HFSS

16. SECURITY CLASSIFICATION OF:			**17. LIMITATION OF ABSTRACT**	**18. NUMBER OF PAGES**	**19a. NAME OF RESPONSIBLE PERSON** Christos E. Maragoudakis
a. REPORT Unclassified	**b. ABSTRACT** Unclassified	**c. THIS PAGE** Unclassified	UU	18	**19b. TELEPHONE NUMBER** *(Include area code)* (575) 678-3145

Standard Form 298 (Rev. 8/98)
Prescribed by ANSI Std. Z39.18

Contents

List of Figures

List of Tables

1. Introduction

Computerized test processes have become an essential part in the testing/evaluation cycle of a system because they quickly identify problematic areas. Once these areas have been identified, further testing in the anechoic chamber can be used to isolate and solve the problem. The development of the antenna radiation pattern models presented in this note is part of a continuous effort to develop a “digital” anechoic chamber in which models can be used to produce preliminary investigations. This effort was performed at the Electromagnetic Vulnerability Assessment Facility (EMVAF) of the U.S. Army Research Laboratory (ARL) Survivability/Lethality Analysis Directorate (SLAD) at White Sands Missile Range (WSMR), NM.

2. Antenna Models

The antenna models for the PENN Engineering WR-284, WR-187, and WR-137 horn antennas were developed using the High Frequency Structure Simulator (HFSS) software developed by Ansoft. The various antenna surfaces were approximated by thin sheets using the “Draw Line” function and then they were joined together using the “Boolean Unite” function to form a single object. Finally, the boundary conditions for the electric field at the antenna surfaces were defined. Furthermore, the excitation of the horn antenna was defined by drawing an additional sheet at the feed of the antenna and identifying it as the “Excitation Wave Port”. The far fields can now be computed by defining a volume in which the wave propagation is to occur. The dimensions of the radiation box must be large enough to meet far field criteria. The computed radiation fields can be displayed in a table form or graphical form.

When the model was used to calculate the radiation pattern, the calculations were performed at points defined by a mesh. The size of the mesh was determined by the frequency used in the computations. The higher the frequency, the finer the mesh used in the computations. When the radiation pattern of an antenna was computed at multiple frequencies simultaneously, the model used the mesh defined by the highest frequency of interest, thus making the mesh very fine, which led to more precise but unnecessary calculations at the lower frequencies. Figure 1 shows the diagram of the HFSS model for the WR-284 horn antenna while figure 2 depicts the modeled radiation pattern of the WR-284 horn antenna at 3.3 gigahertz (GHz).

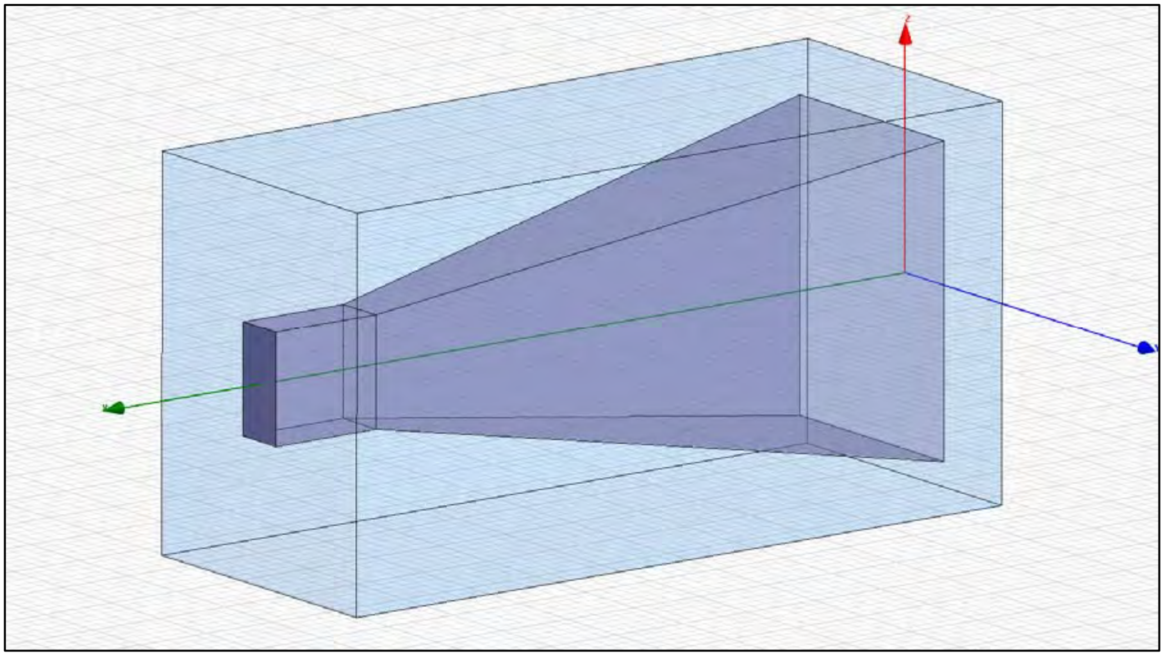

Figure 1. HFSS antenna model for the WR-284 horn antenna.

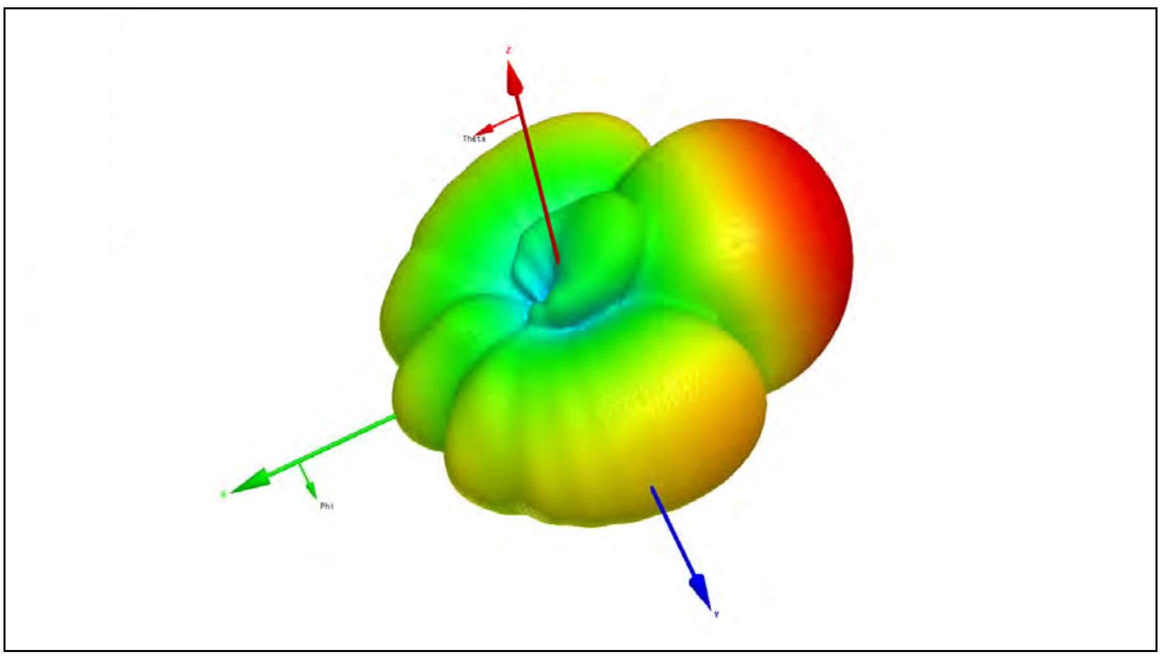

Figure 2. Modeled radiation pattern of WR-284 horn antenna at 3.3 GHz.

3. Validation

The developed models were validated by comparing the modeled data to measured data. The measured data was obtained by measuring the radiation pattern at approximately the center of the operational frequency of each antenna. The measurements were performed at 7.0 GHz, 4.9 GHz and 3.3 GHz for the WR-137, WR-284, and WR-187 horn antennas, respectively. Principal radiation plane (E-plane and H-plane) patterns were measured at 2° increments and then compared to the modeled data. Figure 3 depicts the setup used in the measurement of the antenna patterns while figure 4 shows a graphical comparison of the modeled and measured antenna E-plane patterns for the WR-284 horn antenna at 3.3 GHz. Additional patterns are shown in the appendix.

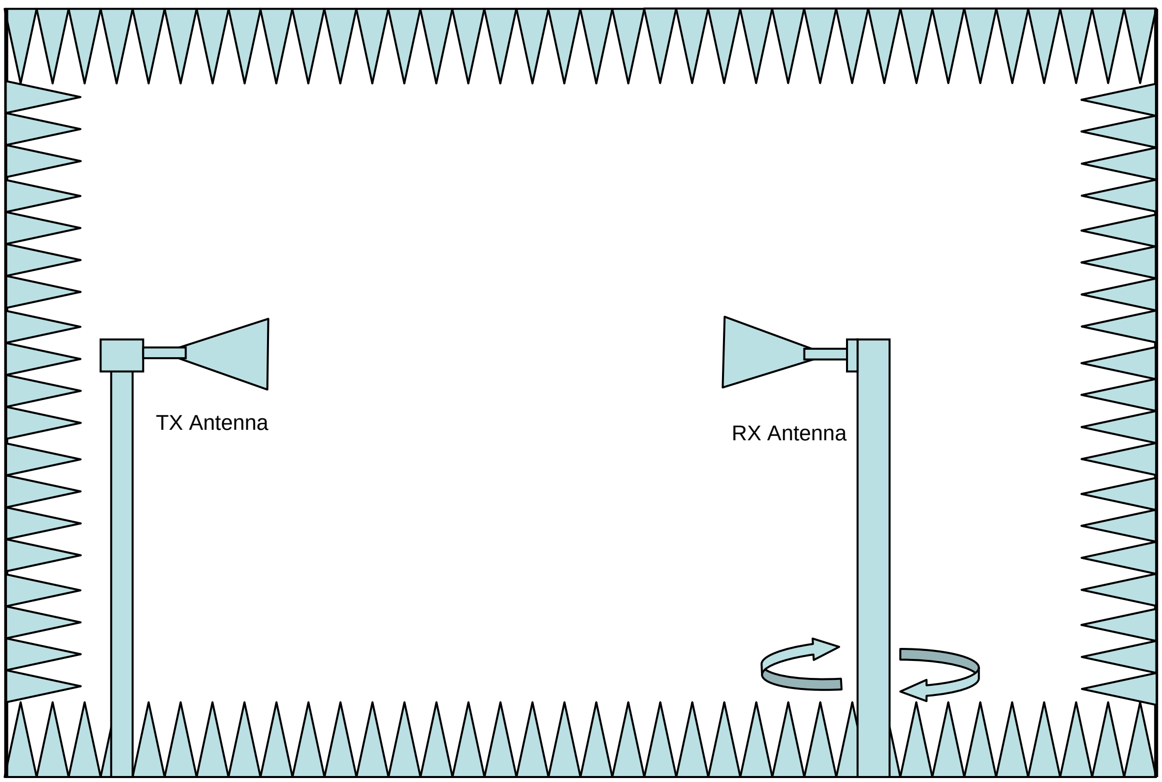

Figure 3. Measurement setup for antenna patterns.

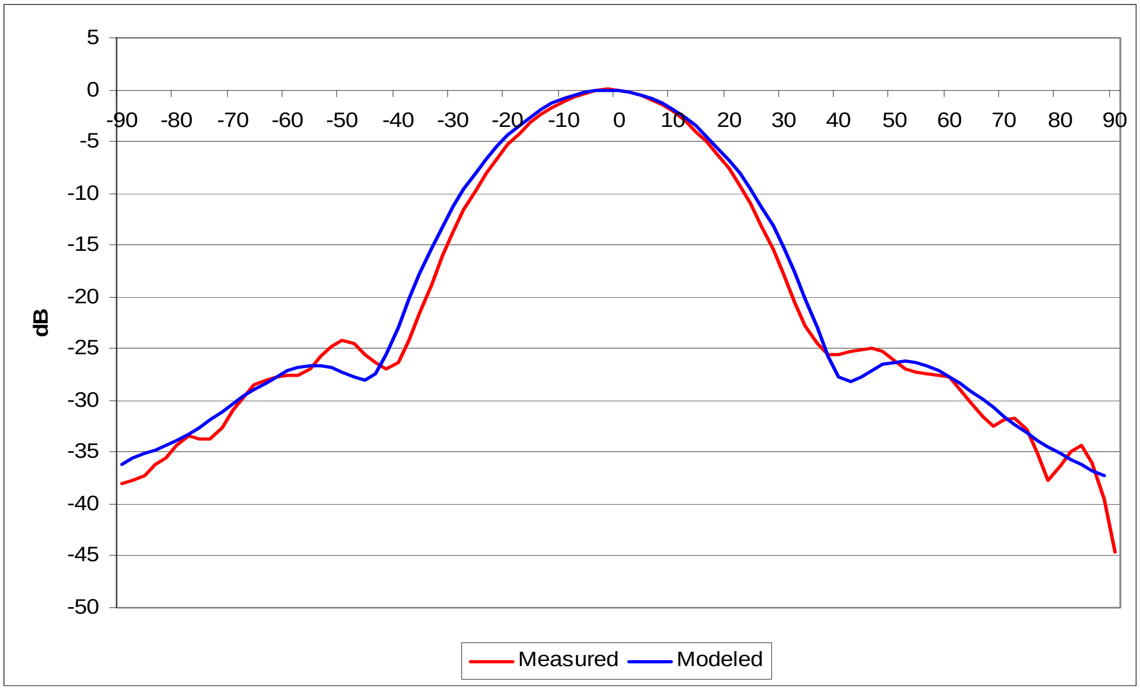

Figure 4. E-plane pattern for WR-284 horn antenna at 3.3 GHz.

The graphical comparisons of the modeled and measured antenna patterns show that patterns of the modeled antennas are wider (larger beamwidth) with deeper nulls. In addition to graphical comparisons, other antenna parameters, such as half-power beamwidth (HPBW), first null beamwidth (FNBW) and sidelobe level (SLL) were compared. Table 1 shows the HPBW in the E-plane and H-plane of the modeled and measured antennas. As it is seen from the table, the HPBW of the modeled antenna pattern is 2° wider than the measured HPBW.

Table 1. Beamwidths of the modeled and measured antennas patterns.

Antenna Model	E-Plane HPBW	H-Plane HPBW
WR-137	—	—
Modeled	32°	32°
Measured	31°	29.5°
WR-187	—	—
Modeled	32°	32°
Measured	30°	30°
WR-284	—	—
Modeled	32°	32°
Measured	30°	30°

The SLL of the measured and modeled patterns is shown in table 2. The SLL of the E-plane modeled patterns is lower compared to the SLL of the measured patterns. The difference varies between 0.4 decibals (dB) at the higher frequency to 2.3 dB at the lower frequency. The H-plane modeled patterns exhibited higher SLL compared to the measured ones. The difference in the SLL varied between 0.2 dB in the lower frequency to 1.1 dB at the higher frequency.

Table 2. SLL levels of the modeled and measured antenna patterns.

Antenna Model	**E-Plane SLL**	**H-Plane SLL**
WR-137	—	—
Modeled	-25.7 dB	-12.9 dB
Measured	-25.3 dB	-14.0 dB
WR-187	—	—
Modeled	-26.5 dB	-12.7 dB
Measured	-24.5 dB	-13.3 dB
WR-284	—	—
Modeled	-26.5 dB	-15.5 dB
Measured	-24.2 dB	-15.3 dB

The FNBW of an antenna is a measure of the resolution capability of an antenna or its ability to resolve two sources. The FNBW for the modeled and measured antenna patterns is shown in table 3.

Table 3. FNBW of the modeled and measured antenna patterns.

Antenna Model	**E-Plane FNBW**	**H-Plane FNBW**
WR-137	—	—
Modeled	88°	76°
Measured	80°	70°
WR-187	—	—
Modeled	96°	76°
Measured	94°	74°
WR-284	—	—
Modeled	88°	76°
Measured	80°	70°

4. Conclusions

Models for three PENN Engineering standard gain horn antennas were developed using the HFSS software and validated using measured data. Comparison between the HPBW, SLL, and FNBW of the modeled and measured radiation patterns show that the modeling of the antennas was successful.

5. Recommendations

SLAD recommends that the antenna modeling and validation be continued to include other type antennas used in the EMVAF. The antennas to be modeled should operate at frequencies other than the ones modeled during this effort. This difference will enhance the library of digital antenna patterns that could be accessed by other simulations.

Appendix. Antenna Patterns

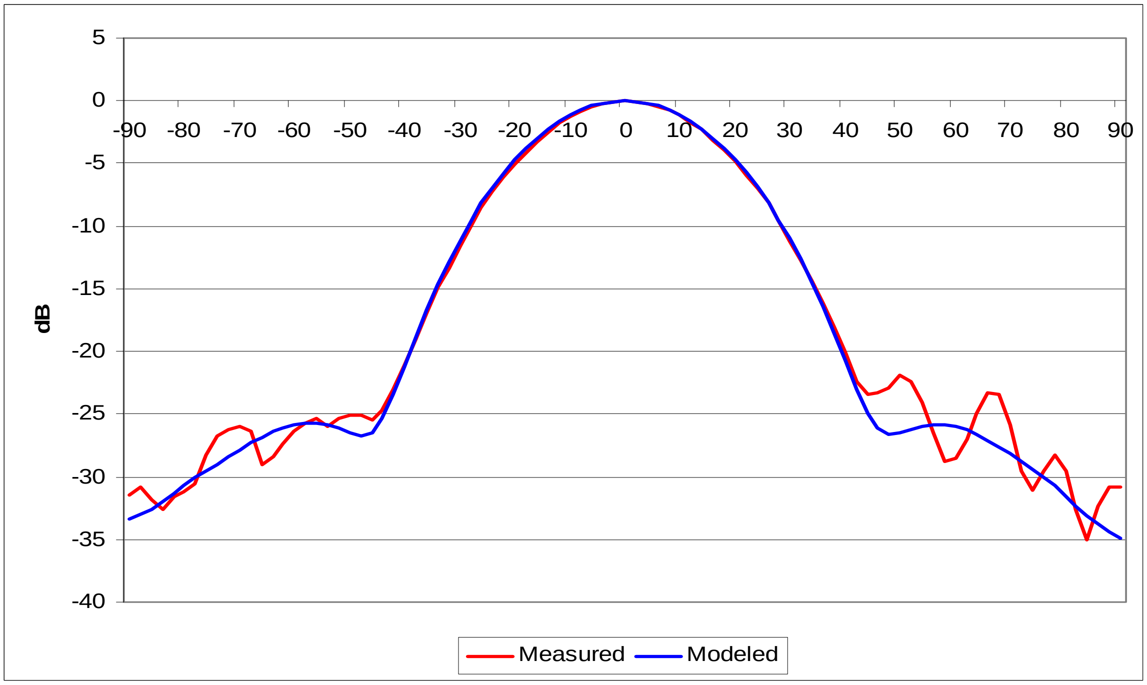

Figure A-1. E-plane pattern for WR-137 horn antenna at 7.0 gigahertz (GHz).

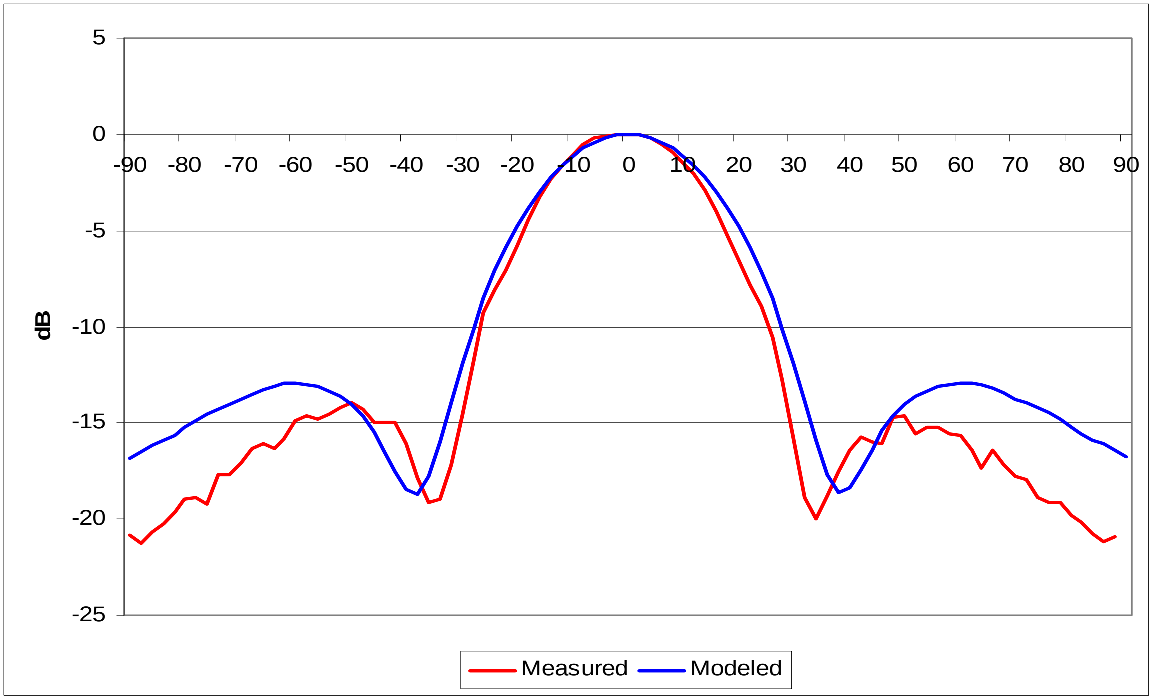

Figure A-2. H-plane pattern for WR-137 horn antenna at 7.0 GHz.

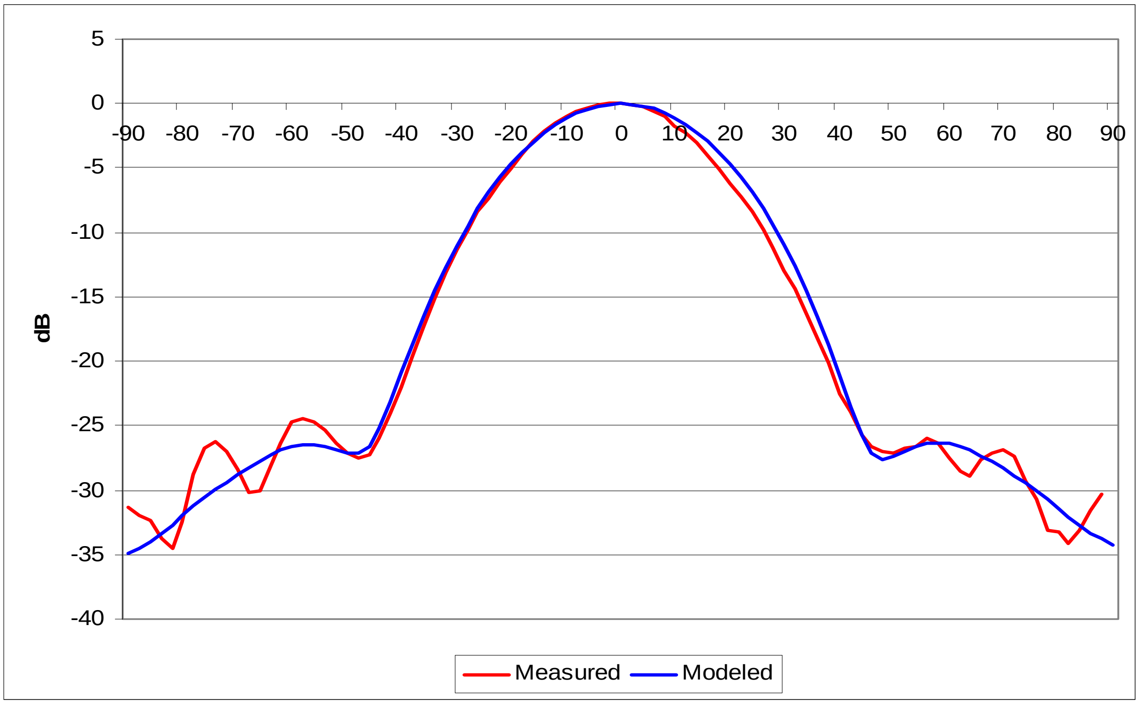

Figure A-3. E-plane pattern for WR-187 horn antenna at 4.9 GHz.

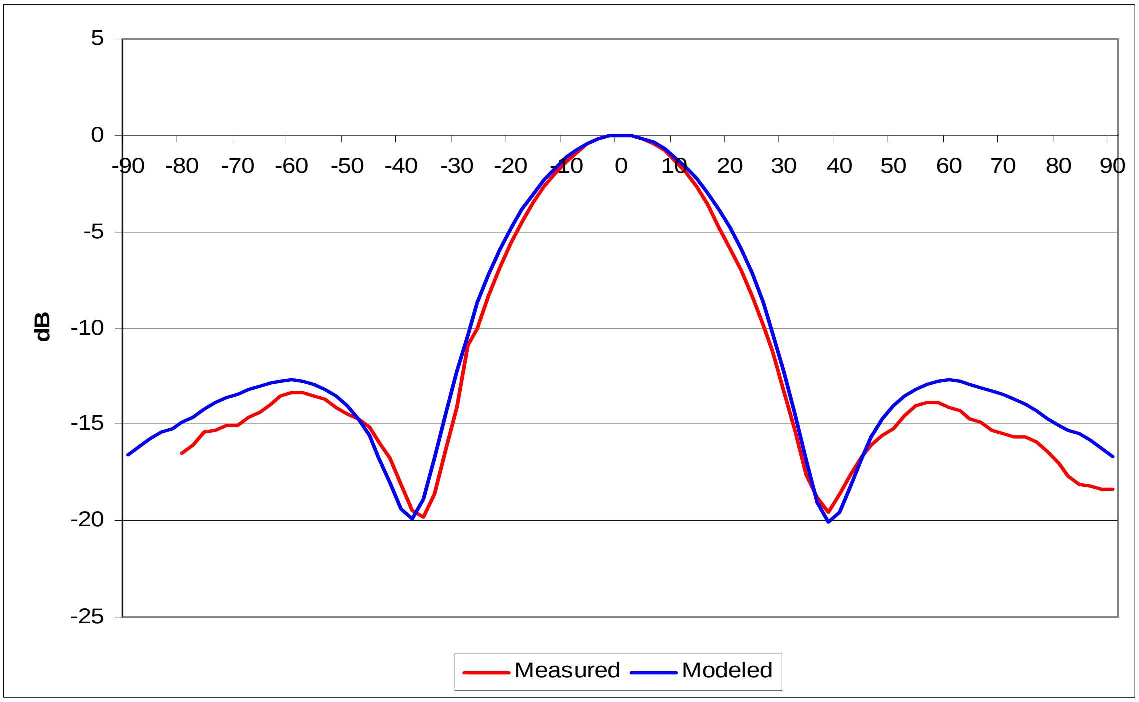

Figure A-4. H-plane pattern for WR-187 horn antenna at 4.9 GHz.

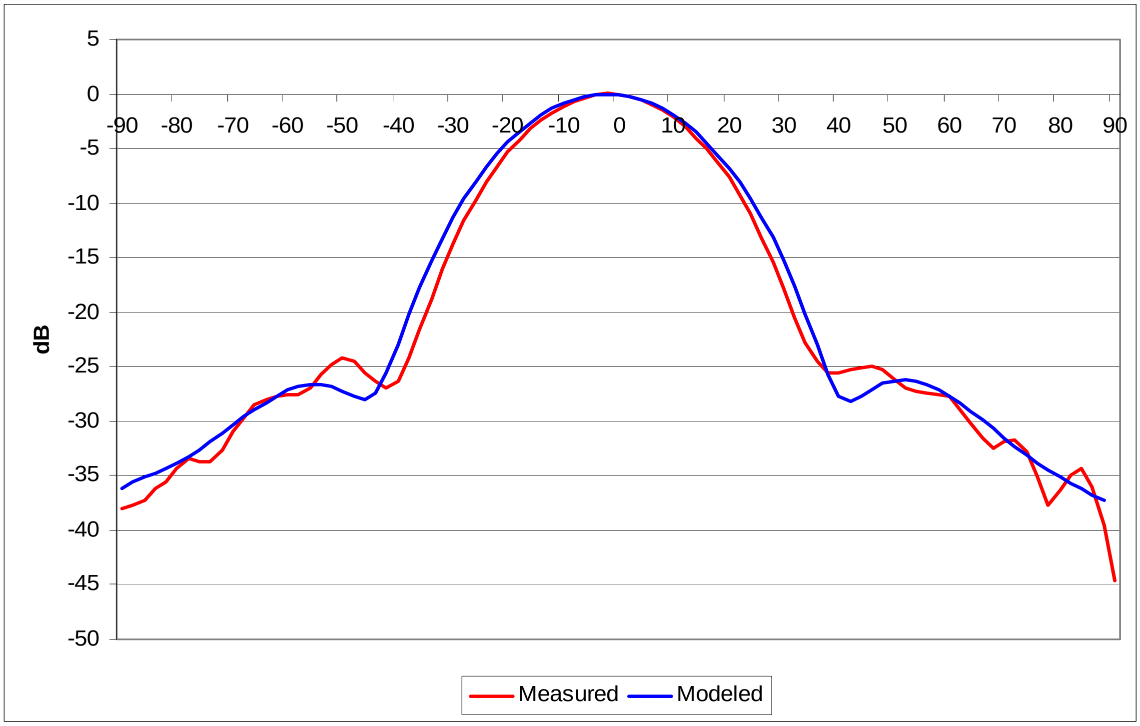

Figure A-5. E-plane pattern for WR-284 horn antenna at 3.3 GHz.

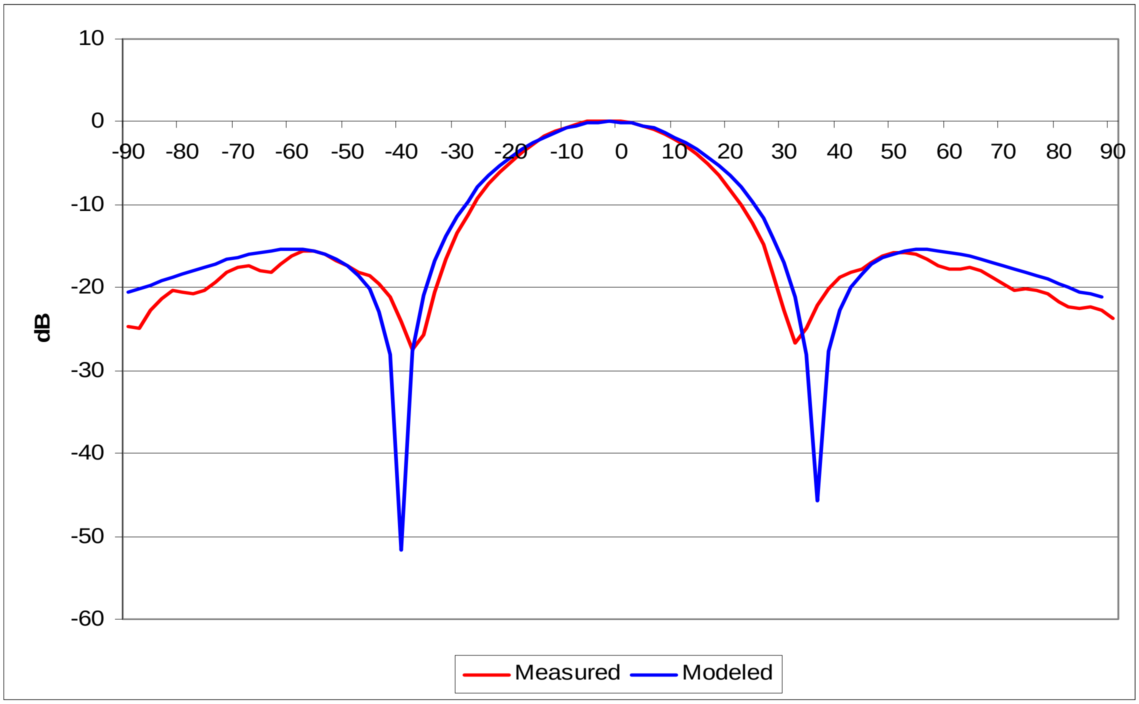

Figure A-6. H-plane pattern for WR-284 horn antenna at 3.3 GHz.

INTENTIONALLY LEFT BLANK.

List of Symbols, Abbreviations, and Acronyms

ARL	U.S. Army Research Laboratory
dB	decibels
EMVAF	Electromagnetic Vulnerability Assessment Facility
FNBW	first null beamwidth
GHz	gigahertz
HPBW	Half-power beamwidth
HFSS	High Frequency Structure Simulator
SLAD	Survivability/Lethality Analysis Directorate
SLL	sidelobe level
WSMR	White Sands Missile Range

No. of Copies	**Organization**
1 PDF	ADMNSTR DEFNS TECHL INFO CTR DTIC OCP 8725 JOHN J KINGMAN RD STE 0944 FT BELVOIR VA 22060-6218
3 HCs	US ARMY RSRCH LAB ATTN RDRL CIM P TECHL PUB ATTN RDRL CIM L TECHL LIB ATTN IMNE ALC HRR MAIL & RECORDS MGMT 2800 POWDER MILL ROAD ADELPHI MD 20783-1197
1 CD	US ARMY RSRCH LAB ATTN RDRL CIM G TECHL LIB BUILDING 4600 APG MD 21005-5066
1 CD 1 WORD VERSION	US ARMY RSRCH LAB MELE ASSOCIATES INC ATTN RDRL SLE E M MORALES BLDG 1622 ROOM 216 WSMR NM 88002-5501
1 HC	US ARMY RSRCH LAB ATTN RDRL SLE S J GONZALEZ BLDG 1624 RM 204 WSMR NM 88002-5513
2 HCs	US ARMY RSRCH LAB ATTN RDRL SLE S C MARAGOUDAKIS BLDG 1628 RM 203 WSMR NM 88002-5513
1 HC	US ARMY RSRCH LAB ATTN RDRL SLE S E REDE BLDG 1628 RM 210 WSMR NM 88002-5513

Total: 11 (1 PDF, 2 CDs, 7 HCs, 1 Word Version)